Physica B 437 (2014) 71–75

Contents lists available at ScienceDirect

Physica B

journal homepage: www.elsevier.com/locate/physb

Spin-dependent Goos–Hänchen shift and spin beam splitter in gate-controllable ferromagnetic graphene

Y. Wang [a], Y. Liu [b,*], B. Wang [a,*]

[a] School of Physics and Engineering, Sun Yat-sen University, Guangzhou 510275, China
[b] School of Engineering, Sun Yat-sen University, Guangzhou 510275, China

ARTICLE INFO

Article history:
Received 6 March 2013
Received in revised form
15 September 2013
Accepted 21 December 2013
Available online 30 December 2013

Keywords:
Goos–Hänchen shift
Spin
Ferromagnetic graphene
Spin beam splitting

ABSTRACT

The transmission and Goos–Hänchen (GH) shift for charge carriers in gate-controllable ferromagnetic graphene induced by ferromagnetic insulator are investigated theoretically. Numerical results demonstrate that spin-up and spin-down electrons exhibit remarkably different transmission and GH shifts. The spin-dependent GH shifts directly demonstrate the spin beam splitting effect, which can be controlled by the voltage of gate. We attribute the spin beam splitting effect to the combination of tunneling through potential barrier and Zeeman interaction from the magnetic field and the exchange proximity interaction between the ferromagnetic insulator and graphene. In view of the spin beam splitting effect and the spin-dependent GH shifts, the gate-controllable ferromagnetic graphene might be utilized to design spin beam splitter.

© 2013 Elsevier B.V. All rights reserved.

1. Introduction

As early as 18th century, Newton put forward that at the interface between two optical mediums with different refraction index totally reflected light deviates the incident light and exhibits a lateral shift [1]. Up to 1940s, Goos and Hänchen experimentally measured the lateral shift and verified Newton′s results. Hence, the lateral shift is named as “Goos–Hänchen (GH) shift” [2]. Afterwards, Artmann and Renard theoretically deduced the formula of GH shift by building the stationary phase method and the energy flux method, respectively [3,4]. The lateral shift is extended to transmitted light across transmitting dielectric layer with positive value figured out by Hsue and Tamir [5] or a slab of denser dielectric medium with negative value pointed out by Li [6]. It has also been shown that GH shift has important application in absorbing dielectric medium, left-handed medium, near-field optics and optic devices [7–11]. The lateral shift is further extended to matter wave [12–23], such as ballistic electrons in the two-dimensional electron gas [15,16] and relativistic Dirac fermions in graphene [17–23].

Since charge carriers in graphene with linear dispersion are different from ballistic electrons in two-dimensional electron gas system with parabolic dispersion [24,25], GH shifts of Dirac fermions in graphene-based medium have some anomalous characteristics and important applications. For example, it is demonstrated that the GH shift at graphene p–n or n–n interface has positive or negative values and leads to twofold spin and valley degeneracies [17]. Furthermore, the GH shift of transmitted electron beams through graphene electrostatic potential barrier can be modulated by the height and width of potential barrier or induced gap [18]. In addition, recent investigations show that the GH shifts in graphene double electrostatic potential barriers or superlattices can be up to the order of electron beam width but are limited inside the transmission gap [19]. Alternatively, the GH shift in graphene can be enhanced in graphene velocity barrier structure by Fabry–Pérot resonance [20]. It is also showed that the GH shifts of totally reflected electron wave at the interface of graphene magnetic barrier or electric magnetic barrier still have spin and valley degeneracies [21]. On the other hand, in view of strain-induced pseudomagnetic fields destroying the valley degeneracy, the strained graphene is used to produce valley-dependent polarized current and demonstrated valley-dependent GH shift [22]. And the valley-dependent lateral displacements of transmitted electron beams through strained graphene region can be designed a valley beam splitter by the valley-dependent GH effect [23].

In this work, we think that if the spin degeneracy is destroyed spin-dependent GH shift in graphene should also happen. Very recently, it is shown that exchange proximity interaction (exchange field) between ferromagnetic insulator and graphene leads to ferromagnetic graphene (FG) with a large exchange-splitting band gap of 5 meV [26], even up to 36 meV in current calculations about magnetic insulator EuO [27]. The exchange-splitting obviously destroys the spin degeneracy in graphene and

* Corresponding authors. Tel.: +86 20 8411 5692; fax: +86 20 8411 3293.
E-mail addresses: stslyl@mail.sysu.edu.cn (Y. Liu), wangbiao@mail.sysu.edu.cn (B. Wang).

0921-4526/$ - see front matter © 2013 Elsevier B.V. All rights reserved.
http://dx.doi.org/10.1016/j.physb.2013.12.032

induces oscillating tunnel magnetoresistance and controllable spin-polarized transports [28–34]. However, up to now, few works have been done on the spin-dependent GH shift. In this paper, we would like to present the spin-dependent GH shift of charge carriers through ferromagnetic graphene. Besides the exchange field, we take into account the confinement effect of magnetic vector potential and the Zeeman interaction from magnetic field induced by the ferromagnetic insulator. It is found that GH shifts of spin-up and spin-down electrons have a remarkable discrepancy and clearly demonstrate the spin splitting effect in this graphene structure.

2. Model and formula

The structure under consideration in Fig. 1 is a monolayer graphene with electrostatic potential barrier, which can be induced by a top or bottom gate [35]. In addition, a magnetic field of $\mathbf{B}=B_0\hat{z}$ with the magnetic field strength B_0 is applied along the z direction perpendicular to graphene and limited within potential barrier region. Such magnetic field can be created by ferromagnetic insulator [36]. Using Landau gauge and $\mathbf{B}=\nabla\mathbf{A}$, we can obtain the corresponding vector potential $\mathbf{A}=(0,\ A(x),\ 0)$, with $A(x)$ satisfying the following expression:

$$A(x)=\begin{cases}0,(x<0),\\ B_0\,x,(0\le x\le d),\\ B_0\,d,(x>d),\end{cases}$$

In this graphene system, the low energy excitation quasiparticles obey the following Dirac–Weyl equation

$$\left[v_F\ \boldsymbol{\sigma}\cdot(-i\hbar\nabla+e\mathbf{A})+V\hat{I}+H_{spin}\hat{I}\pm H_{ex}\hat{I}\right]\boldsymbol{\psi}=E\boldsymbol{\psi},\tag{1}$$

where $\boldsymbol{\sigma}=(\boldsymbol{\sigma}_x,\ \boldsymbol{\sigma}_y)$ is the Pauli matrix vector, V is the electrostatic potential induced by the gate, $\hat{I}$ is the unit matrix, $H_{spin}=1/2\mu_B gsB_0$ is the Zeeman interaction term with the Bohr magneton (μ_B), the Landé factor ($g\approx 2$) and the spin orientation s and H_{ex} is the exchange field. In this work, $s=1$ and $s=-1$ denote parallel and antiparallel relations between the spin orientation and the direction of magnetic field, respectively. Due to the invariance of momentum along the y direction, the four-component wave function can be written as

$$\boldsymbol{\psi}(\mathbf{r})=\left[\psi_{A\uparrow}(x),\psi_{B\uparrow}(x),\psi_{A\downarrow}(x),\psi_{B\downarrow}(x)\right]^T\exp(ik_y y),\tag{2}$$

where A (B) denotes the sublattice of graphene and ↑(↓) denotes the spin up (down) of electron. To simplify the expression and calculation, we can conveniently introduce following dimensionless units: $x\to L_B x$, $\mathbf{A}\to L_B B_0\mathbf{A}$, $k_y\to 1/L_B k_y$, $V\to E_0 V$ and $E\to E_0 E$, where $L_B=\sqrt{\hbar/eB_0}$ is the length scale and $E_0=\hbar v_F/L_B$ is the energy scale with $k_F=E/\hbar v_F$. Thus, the Zeeman interaction term and the exchange field can be combined and rewritten as $H_{spin}\pm H_{ex}\approx s\lambda E_0\Theta(d/2-|x|)$, where Θ is the step function and λ varies from 0.002 with a Zeeman field of 1 T up to 0.2 in the case of exchange splitting of 5 meV [26,32]. By solving Eq. (1), we can obtain the wave functions in three regions in Fig. 1(b).

For regions (i) and (iii), the wave functions are

$$\boldsymbol{\psi}_{\mathrm{I}}(x)=\boldsymbol{\Omega}_{\mathrm{I}}(x)\begin{bmatrix}1\\ r_{ss'}\end{bmatrix},\tag{3a}$$

$$\boldsymbol{\Omega}_{\mathrm{I}}(x)=\begin{bmatrix}\exp(ik_x^i x) & \exp(-ik_x^i x)\\ \frac{k_x^i+ik_y}{E}\exp(ik_x^i x) & \frac{-k_x^i+ik_y}{E}\exp(-ik_x^i x)\end{bmatrix},\tag{3b}$$

$$\boldsymbol{\psi}_{\mathrm{III}}(x)=\boldsymbol{\Omega}_{\mathrm{III}}(x)\begin{bmatrix}\sqrt{k_x^i/k_x^f}\,t_{ss'}\\ 0\end{bmatrix},\tag{3c}$$

$$\boldsymbol{\Omega}_{\mathrm{III}}(x)=\begin{bmatrix}\exp(ik_x^f x) & \exp(-ik_x^f x)\\ \frac{k_x^f+i(k_y+B_0 d)}{E}\exp(ik_x^f x) & \frac{-k_x^f+i(k_y+B_0 d)}{E}\exp(-ik_x^f x)\end{bmatrix},\tag{3d}$$

where $k_x^i=\sqrt{E^2-k_y^2}$ and $k_x^f=\sqrt{E^2-(k_y+B_0 d)^2}$ are corresponding longitude wave vectors in incident and exist regions and $r_{ss'}$ and $t_{ss'}$ are the corresponding reflection and transmission coefficients for an incident quasiparticle wave with spin s as well as reflected (transmitted) wave with spin s'. Note that the factor $\sqrt{k_x^i/k_x^f}$ in Eq. (3c) ensures the normalization of probability current. Corresponding incident and exit angles are $\theta=\arctan(k_y/k_x^i)$ and $\phi=\arctan[(k_y+B_0 d)/k_x^f]$, respectively.

For the middle region (ii), the wave functions satisfying Eq. (1) can be written as a linear combination of the Weber functions [36,37], as follow:

$$\boldsymbol{\psi}_{\mathrm{II}}(x)=\boldsymbol{\Omega}_{\mathrm{II}}(x)\begin{bmatrix}\alpha\\ \beta\end{bmatrix},\tag{4a}$$

$$\boldsymbol{\Omega}_{\mathrm{II},\ B>0}(x)=\begin{bmatrix}D_{p_s}(q) & D_{p_s}(-q)\\ \frac{i\sqrt{2}}{E-V-s\lambda}D_{p_s+1}(q) & \frac{-i\sqrt{2}}{E-V-s\lambda}D_{p_s+1}(-q)\end{bmatrix},\tag{4b}$$

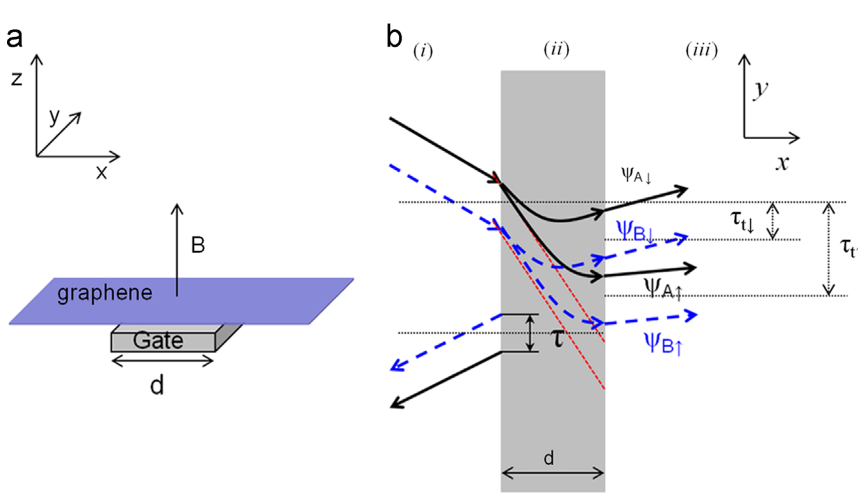

Fig. 1. (a) Schematic of gate-controlled ferromagnetic graphene with magnetic field. (b) Spin-dependent GH shifts are presented in this configuration, where dash lines denote the refracted beams without magnetic field and τ is the relative displacement between upper (solid arrow line) and lower (dash arrow line) components.

$$\mathbf{\Omega}_{\text{II},\ B<0}(x) = \begin{bmatrix} D_{p_s+1}(-q) & D_{p_s+1}(q) \\ \frac{-i\sqrt{2}}{E-V-s\lambda}(p_s+1)D_{p_s}(-q) & \frac{i\sqrt{2}}{E-V-s\lambda}(p_s+1)D_{p_s}(q) \end{bmatrix}, \quad (4c)$$

where α and β are complex coefficients and $D_p(q)$ is the parabolic cylinder function with $q=\sqrt{2}[k_y+B_0x]$ and $p_s=E-s\lambda^2/2-1$.

Using the continuity of wave functions and Eqs. (3a)–(4c), we can obtain the reflection coefficient $r_{ss'}(k_y)=|r_{ss'}(k_y)|\exp[i\mu_r(k_y)]$ and the transmission coefficient $t_{ss'}(k_y)=|t_{ss'}(k_y)|\exp[i\mu_t(k_y)]$, with reflection phase $\mu_r(k_y)$ and transmission phase $\mu_t(k_y)$. Afterwards, according to the stationary-phase approximation [3], we can obtain the spin-dependent GH shifts for the upper and lower reflected and transmitted beams at $k_y=k_{y0}$, as follow:

$$\tau^{\pm}_{r,ss'} = -d\mu_r/dk_y|_{k_y=k_{y0}} \mp \tau, \quad (5a)$$

$$\tau^{\pm}_{t,ss'} = -d\mu_t/dk_y|_{k_y=k_{y0}}, \quad (5b)$$

where τ is the relative displacement between upper and lower components [17], as shown in Fig. 1(b). The average shifts of $\tau_{r,ss'}=(\tau^{+}_{r,\ ss'}+\tau^{-}_{r,\ ss'})/2$ and $\tau_{t,ss'}=(\tau^{+}_{t,ss'}+\tau^{-}_{t,ss'})/2$ are independent of the relative displacement τ and used to denote the spin-dependent GH shifts of reflected and transmitted beams, respectively.

3. Results and discussions

Fig. 2 shows the transmission ($T=|t_{ss'}{}^2|$) and GH shift of Dirac fermions versus the incident energy in graphene structure, at some specific incident angles of $\theta=5^\circ$, $\theta=10^\circ$ and $\theta=15^\circ$. The physic parameters of the structure are taken as $d=1$, $B=1$, $V=3$. In this work, λ is chosen as 0.2, with respect to the exchange splitting of 5 meV. A transmission gap exists and the width of the gap becomes wider with increasing the incident angle, as shown in Fig. 2(b). The direction-dependent transmission gap arises from the magnetic confinement, which has been previously figured out and suggested as direction-dependent filter [36,37]. In addition, it can be seen from Fig. 2(a) that at the edge of transmission gap the GH shift has a peak related to the total reflection and is previously discussed in magnetic barrier [21]. However, a more obvious result in Fig. 2(a) shows that GH shifts of spin-up and spin-down electrons have a remarkable discrepancy. This is to say, the spin splitting for transmitted electron beams appears in such a graphene device. Such spin splitting arises from the combination of the tunneling through the electrostatic potential barrier, the Zeeman interaction induced magnetic field and the exchanging field. With increasing the incident energy, the spin-dependent GH shift first increases dramatically, then reaches a resonant maximum, and finally keeps relatively stable. In other word, the spin-dependent GH shifts are highly dependent on the incident energy and the incident direction. As shown in Fig. 2(a), the GH shifts for the spin-up and spin-down transmitted electron beams are obviously enhanced with increasing the incident angle.

Usually, the difference $\Delta\tau_t=\tau_{t\uparrow}-\tau_{t\downarrow}$ between the spin-up and spin-down GH shifts can be defined as the spin polarization, which denotes the degree of spin splitting. Fig. 3 shows the spin polarization of the GH shifts as a function of the incident energy, with the same structure parameters in Fig. 2. It can be clearly observed that transmitted electron beams through this configuration exhibit considerable spin polarization effect. With increasing the incident energy, the spin polarization varies dramatically from negative to positive values. In addition, the bigger the incident angle is, the more obvious the spin polarization becomes. In other words, the splitting of transmitted spin electron beams can be enhanced by increasing the incident angle.

As previously mentioned, the magnitude of potential barrier can be tuned by the voltage of top or bottom gate. Fig. 4 shows the spin-dependent transmission and GH shift as functions of the incident energy, with some specific voltages of $V=-1.5$, 1.5 and 2.5. In this calculation, the structure parameters and the incident angle are taken as $d=1$, $B=1$ and $\theta=15^\circ$. The edge of transmission gap is scarcely influenced by the potential barrier, but the transmission is obviously suppressed if the electrostatic potential is positive. The spin splitting is obviously enhanced in the case of potential barrier ($V=1.5$ and 2.5). This means that transmission tunneling appears through potential barrier ($V>0$). On the contrary, the transmission tunneling and spin splitting are not obvious in the case of potential well ($V=-1.5$). Again, we can conclude that spin splitting should be attributed to the combination of tunneling through the electrostatic potential barrier, the Zeeman interaction and the exchanging filed. The spin polarization of GH shifts induced by the combined interaction is more clearly presented in Fig. 5, with the same structure parameters in Fig. 4. One can clearly observe the spin polarization in the presence of electrostatic potential barriers with $V=1.5$ and 2.5, owing to the electronic tunneling through potential barrier, which is absent in potential well with $V=-1.5$.

In order to further evaluate the effect of electrostatic potential on the spin-dependent GH shifts and the spin polarization, we calculate the GH shift and the spin polarization as functions of the height of electrostatic potential barrier and plot the results in

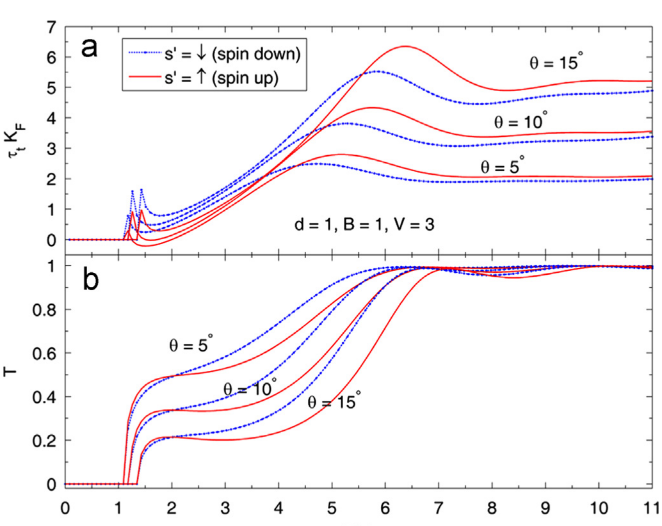

Fig. 2. Spin-dependent GH shifts (a) and transmission (b) as functions of energy E at some specific angles.

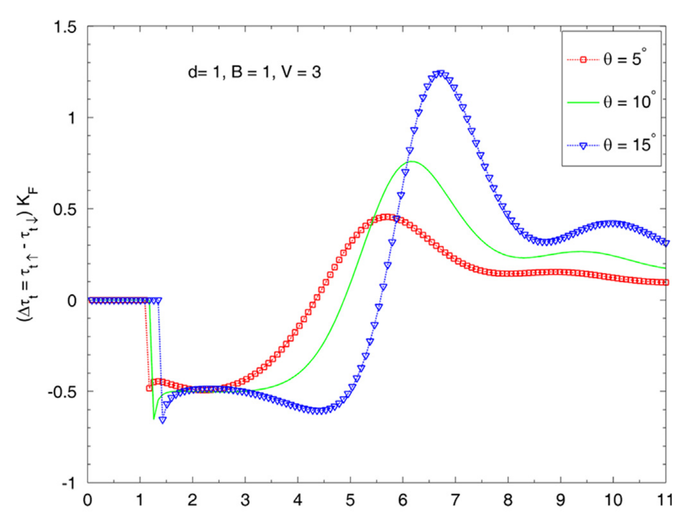

Fig. 3. Spin polarization of GH shifts as a function of energy E at some specific angles with the same structure in Fig. 2.

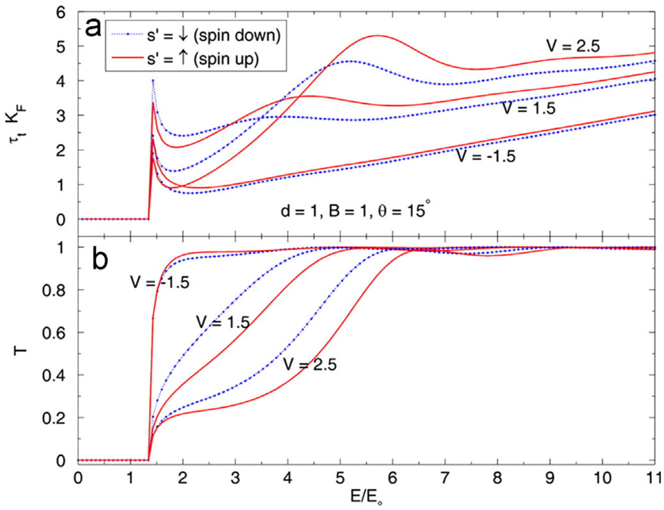

Fig. 4. Spin-dependent GH shifts (a) and transmission (b) as functions of energy E with some specific voltages at the incident angle $\theta = 15^\circ$.

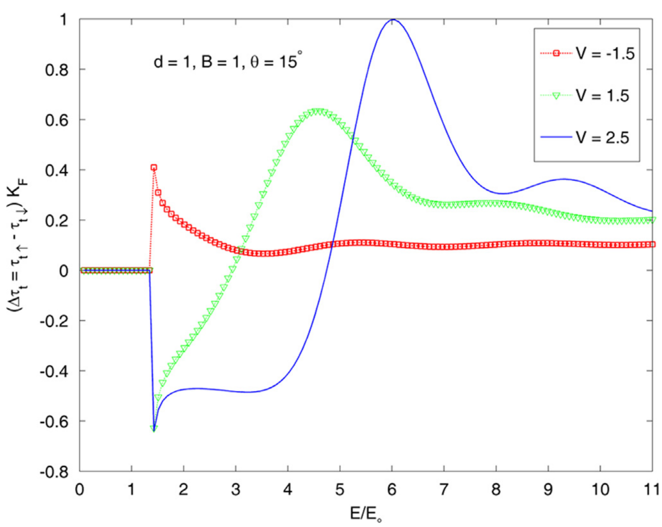

Fig. 5. Spin polarization of GH shifts as a function of energy E with some specific voltages and the same structure in Fig. 4 at the incident angle $\theta = 15^\circ$.

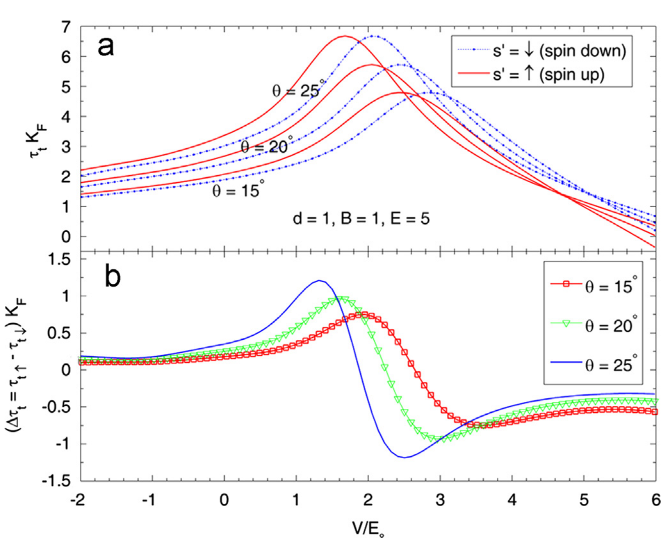

Fig. 6. Spin-dependent GH shifts (a) and spin polarization of GH shifts (b) as functions of voltage at some specific angles.

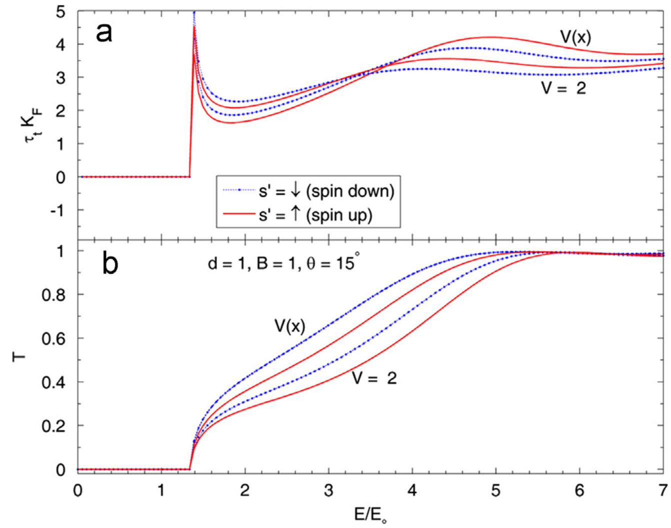

Fig. 7. Spin-dependent GH shifts (a) and transmission (b) as functions of energy E at the incident angle $\theta = 15^\circ$, for rectangle potential barrier $V = 2$ and barrier with potential profile $V(x)$.

Fig. 6. The physic parameters are taken as $d = 1$, $B = 1$ and $E = 5$. Indeed, from Figs. 6(a) and (b), it can be seen that the spin splitting is very weak in the case of $V < 0$. As long as the electrostatic potential is positive, the spin-dependent GH shifts vary dramatically and the spin polarization becomes quite obvious. That means that one can control the spin splitting by adjusting the applied voltage of the top or bottom gate. In other words, the configuration may be used as gate-controllable spin beam splitter.

Finally, we evaluate the effect of potential barrier smoothness on the GH shifts and the spin polarization for transmitted electron beams through the barrier, where a typical potential profile of $V(x) = 0.5V[erf(2x/w-2) + erf(2(w-x)/w-2)]$ is used with $w = 0.1d$ and $erf(x)$ as the error function [23]. Fig. 7 shows the transmission and GH shift versus incident energy with structure parameters of $d = 1$, $V = 2$ and $B = 1$, at specific incident angle of $\theta = 15^\circ$. The spin-dependent GH shifts and the spin splitting of transmitted electron beams remain in this structure. Thus, gate-controlled graphene with magnetic field induced by ferromagnetic insulator can be suggested as spin beam splitter.

4. Conclusion

In summary, we have investigated the spin-dependent transmission and quantum GH shifts for Dirac fermions through gate-controlled ferromagnetic graphene produced by ferromagnetic insulator. Owing to the combined interaction of tunneling through electrostatic potential barrier, Zeeman interaction of magnetic field and the exchange field between graphene and ferromagnetic insulator, a remarkable spin splitting effect between spin-up and spin-down electrons in graphene occurs. The distance of spin splitting is clearly demonstrated by the difference between the GH shifts of spin-up and spin-down electrons and can be controlled by the voltage of gate. Such spin splitting can be used to realize controllable spin beam splitter, which plays an important role in spin-polarized source, spin injection and detection and spin-dependent transport in graphene spintronics [38–42].

Acknowledgments

This work was supported by the National Natural Science Foundation through the funds (Nos. 11232015, 11072271), and the Research Fund for the Doctoral Program of Higher Education of China (No. 20120171110005).

References

[1] I. Newton, Opticks: A Treatise of the Reflexions, Refractions, Inflexions and Colors of Light, Royal Society, London, 1704.
[2] F. Goos, H. Hänchen, Ann. Phys. 436 (1947) 333; F. Goos, H. Hänchen, Ann. Phys. 440 (1949) 251.
[3] K.V. Artmann, Ann. Phys. 2 (1948) 87.
[4] R.H. Renard, J. Opt. Soc. Am. 54 (1964) 1190.
[5] C.W. Hsue, T. Tamir, J. Opt. Soc. Am. A 2 (1985) 978.
[6] C.F. Li, Phys. Rev. Lett. 91 (2003) 133903.
[7] T. Sakata, H. Togo, F. Shimokawa, Appl. Phys. Lett. 76 (2000) 2814.
[8] X. Chen, C.F. Li, Phys. Rev. E 69 (2004) 066617.
[9] L.G. Wang, H. Chen, S.Y. Zhu, Opt. Lett. 30 (2005) 2936.
[10] X. Yin, L. Hesselink, Appl. Phys. Lett. 89 (2006) 261108.
[11] Y. Wang, Z. Cao, H. Li, J. Hao, T. Yu, Q. Shen, Appl. Phys. Lett. 93 (2008) 091103.
[12] J.L. Carter, H. Hora, J. Opt. Soc. Am. 6 (1971) 1640.
[13] V.K. Ignatovich, Phys. Lett. A 322 (2004) 36.
[14] V.O. de Haan, J. Plomp, T.M. Rekveldt, W.H. Kraan, A.A. van Well, R.M. Dalgliesh, S. Langridge, Phys. Rev. Lett. 104 (2010) 010401.
[15] X. Chen, C.-F. Li, Y. Ban, Phys. Rev. B **77** (2008) 073307.
[16] X. Chen, X.J. Lu, Y. Wang, C.F. Li, Phys. Rev. B 83 (2011) 195409.
[17] C.W.J. Beenakker, R.A. Sepkhanov, A.R. Akhmerov, J. Tworzydło, Phys. Rev. Lett. 102 (2009) 146804.
[18] X. Chen, J.-W. Tao, Y. Ban, Eur. Phys. J. B 79 (2011) 203.
[19] Y. Song, H.-C. Wu, Y. Guo, Appl. Phys. Lett. 100 (2012) 253116; X. Chen, P. Zhao, X. Lu, Eur. Phys. J. B 86 (2013) 223.
[20] Y. Wang, Y. Liu, B. Wang, Physica E 48 (2013) 191; Y. Wang, Y. Liu, B. Wang, Physica E 53 (2013) 186.
[21] Y. Wang, Y. Liu, B. Wang, Superlattices Microstruct. 60 (2013) 240; M. Sharma, S. Ghosh, J. Phys.: Condens. Matter 23 (2011) 055501.
[22] Z. Wu, F. Zhai, F.M. Peeters, H.Q. Xu, K. Chang, Phys. Rev. Lett. 106 (2011) 176802.
[23] F. Zhai, Y. Ma, K. Chang, New J. Phys. 13 (2011) 083029.
[24] K.S. Novoselov, A.K. Geim, S.V. Morozov, D. Jiang, Y. Zhang, S.V. Dubonos, I.V. Grigorieva, A.A. Firsov, Science 306 (2004) 666.
[25] K.S. Novoselov, A.K. Geim, S.V. Morozov, D. Jiang, M.I. Katsnelson, I.V. Grigorieva, S.V. Dubonos, A.A. Firsov, Nature 438 (2005) 197.
[26] H. Haugen, D. Huertas-Hernando, A. Brataas, Phys. Rev. B **77** (2008) 115406.
[27] H.X. Yang, A. Hallal, D. Terrade, X. Waintal, S. Roche, M. Chshiev, Phys. Rev. Lett. 110 (2013) 046603.
[28] Z.P. Niu, F.X. Li, B.G. Wang, L. Sheng, D.Y. Xing, Eur. Phys. J. B 66 (2008) 245.
[29] T. Yokoyama, Phys. Rev. B 77 (2008) 073413.
[30] C. Bai, X. Zhang, Phys. Lett. A 372 (2008) 725.
[31] B. Soodchomshom, I.M. Tang, R. Hoonsawat, Phys. Lett. A 372 (2008) 5054.
[32] L. Dell′Anna, A. De Martino, Phys. Rev. B 80 (2009) 155416.
[33] J. Zou, G. Jin, Y. Ma, J. Phys, Condens. Matter 21 (2009) 126001.
[34] T. Yokoyama, J. Linder, Phys. Rev. B 83 (2011) 081418.
[35] B. Özyilmaz, P. Jarillo-Herrero, D. Efetov, D.A. Abanin, L.S. Levitov, P. Kim, Phys. Rev. Lett. 99 (2007) 166804.
[36] M. Ramezani Masir, P. Vasilopoulos, A. Matulis, F.M. Peeters, Phys. Rev. B **77** (2008) 235443.
[37] A. De Martino, L. Dell′ Anna, R. Egger, Phys. Rev. Lett. 98 (2007) 066802.
[38] E.W. Hill, A.K. Geim, K. Novoselov, F. Schedin, P. Blake, IEEE Trans. Magn. 42 (2006) 2694.
[39] S. Cho, Y.F. Chen, M.S. Fuhrer, Appl. Phys. Lett. 91 (2007) 123105.
[40] N. Tombros, C. Jozsa, M. Popinciuc, H.T. Jonkman, B.J. van Wees, Nature 448 (2007) 571.
[41] W. Han, K. Pi, K.M. McCreary, Y. Li, J.J.I. Wong, A.G. Swartz, R.K. Kawakami, Phys. Rev. Lett. 105 (2010) 167202.
[42] H. Zhang, H. Jiang, X.C. Xie, Q.F. Sun, Phys. Rev. B 83 (2011) 155402.